X-ray structure of Cs-doped polyacetylene

J. Ma,* D. Djurado,† and J. E. Fischer‡
Laboratory for Research on the Structure of Matter, University of Pennsylvania, Philadelphia, Pennsylvania 19104

N. Coustel and P. Bernier
Groupe de Dynamique des Phases Condensées, Université des Sciences et Techniques du Languedoc, 34060 Montpellier CEDEX, France

(Received 7 August 1989)

The x-ray powder profile of heavily doped $[(CH)Cs_y]_x$ is analyzed on the basis of three dimensionally ordered intercalate channels. Fifteen peaks representing 27 unique reflections are well described (positions and intensities) by a tetragonal pseudocell with $\bar{a}=\bar{b}=9.093$ Å, $\bar{c}=7.950$ Å containing 24 (CH) and 4 Cs units ($y=0.167$). The Cs and (CH) sublattices are actually incommensurate along $\bar{c}$, with 6.46 undistorted (CH) units per Cs implying $y=0.15$. Reflections with nonzero L are significantly less intense than calculated neglecting the Debye-Waller factor, indicating large-amplitude c-axis thermal motion of Cs ions. The fractional linear in-plane dilation upon replacing K with Cs is within 20% of the corresponding value in graphite intercalates.

Polyacetylene doped with alkali metals continues to attract interest as a prototype system for understanding the structure of conducting polymers. Several recent studies have confirmed the basic features of the channel structure first proposed by Shacklette[1] and have added important new information. For the case of sodium doping, Winokur *et al.* found that the two-dimensional (2D) triangular superlattice of channels is incommensurate over a concentration range of 6–10%.[2] Djurado *et al.* showed that potassium doping proceeds via selective filling of the two unique channels in a centered 2D square superlattice, and that the staging transitions correlate with steps in the charge-discharge curves as expected on simple thermodynamic grounds.[3] Using film techniques on highly oriented samples doped with K, Rb, and Cs, Saldi *et al.* showed that the metal sublattice exhibits 3D long-range order.[4] We have undertaken an x-ray measurement of $[(CH)Cs_y]_x$ doped to saturation ($y\sim0.16$) by the vapor-phase method; we present here a three-dimensional structural model for this phase, based on an x-ray-diffraction profile with 15 peak positions and intensities well accounted for. Comparing the lattice parameters with our previous $[(CH)K_y]_x$ data, we find systematic differences relating to the ionic diameter which can be compared to the analogous graphite layer intercalates.

Our sample was prepared from unoriented Shirakawa $(CH)_x$. A single film 200-μm thick was first isomerized at 180°C for 1 h under dynamic vacuum, then loaded into one end of a 10-mm-diameter glass tube with a 20-mm-diameter thin-wall bubble designed to minimize glass absorption and scattering. The film was firmly centered in the bubble by a stainless-steel support. Cesium metal was distilled into the opposite end of the tube, which was then sealed off under dynamic vacuum. Doping was carried out with the Cs reservoir at 200°C and the $(CH)_x$ at 210°C for 24 h. Two advantages of this procedure are: no possibility for cointercalation of solvent, and no need for glove-box manipulation between synthesis and x-ray measurement. A much larger sample similarly prepared showed no nuclear magnetic resonance (NMR) evidence for metallic cesium.[5] X-ray data were taken mainly in the transmission mode, using a highly focused monochromatic beam from a Mo rotating anode operating at 10 kW. This closely approximates Debye-Scherrer geometry, with negligible sample absorption corrections. Reflection-mode scans were performed over a limited-Q range to verify the absence of preferred orientation in our sample. Details of the setup have been described previously.[3]

Figure 1(a) shows the overall diffractogram, while Fig. 1(b) gives an expanded view of the weaker high-Q peaks. Four strong reflections are observed in the range $0.7<Q<2.3$ Å^{-1}; weaker peaks occur at 1.4 Å^{-1} and extend up to 4.5 Å^{-1}. The background is composed mainly of air scattering (decreasing slowly with Q) and diffuse scattering from the glass bubble (broadly peaked at 1.6 Å^{-1}). The sharp drop in intensity above 2.3 Å^{-1} is a characteristic feature of the structure, as described below. Figure 1(b) confirms the absence of preferred orientation and validates an intensity analysis based on Debye-Scherrer calculations; in oriented $(CH)_x$ with the average $\bar{c}$ vector in the scattering plane, a transmission scan ("meridional") would emphasize the L component while the reflection scan ("equatorial") would favor the (H,K) components. The weaker peaks at high Q are better defined in the reflection scan; many of these arise from overlapping reflections, as discussed below. All peaks which can be assigned to a single reflection have the same Q widths within experimental error; by assigning Gaussian line shapes we estimate the correlation length to be 80 Å.

For the initial indexing we considered only the Cs sublattice. A simple 2D square lattice of Cs channels projected onto the (a,b) plane requires that the first peak at

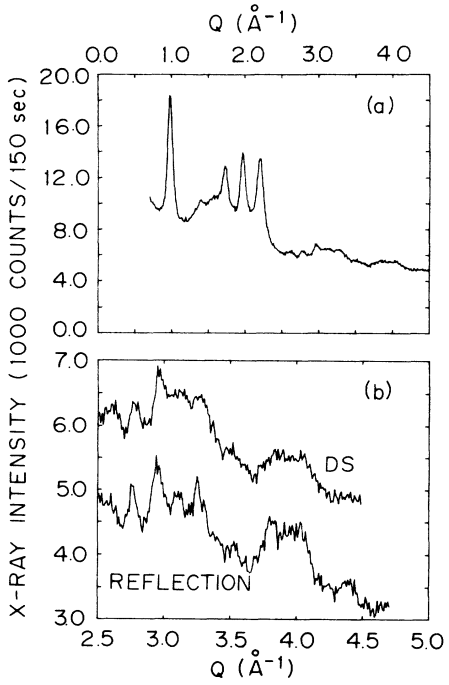

FIG. 1. Powder x-ray profiles of Cs-doped $(CH)_x$. (a) Debye-Scherrer geometry (DS), overall view. (b) Expanded view of weak peaks at high Q; comparison of DS and flat-plate-reflection geometries (the profiles are offset for clarity).

0.977 Å^{-1} be the (100) reflection and $\bar{a}=6.431$ Å. This assumption accounts for many of the observed peaks but also leaves out some, in particular the strong peak at 1.725 Å^{-1} which coincides with the (020)/(110) doublet of undoped *trans*-$(CH)_x$ (1.71 and 1.76 Å^{-1}, respectively) and thus might indicate a sizeable fraction of undoped $(CH)_x$ in the bulk of the film. We can rule out this possibility because (a) the large intensity indicates that the Cs form factor must be involved in this reflection; (b) the peak does not show the (020)/(110) splitting which would be expected for 80-Å correlation length and the high Q resolution employed; and (c) even if the doublet were washed out due to smaller correlation length for the undoped phase (an unlikely possibility), the observed width is too small for a composite peak whose components are separated by 0.05 Å^{-1}.

We next considered two 3D structures, face-centered and body-centered tetragonal (fct and bct), in which the 1.725-Å^{-1} peak would be an (HKL) reflection with nonzero L; in either case the first peak at 0.977 Å^{-1} must be the (110), hence $\bar{a}=9.093$ Å. In the fct model the 1.725-Å^{-1} peak is the (001) and $\bar{c}=3.642$ Å, while for the bct model the 1.725-Å^{-1} peak is the (101) and $\bar{c}=3.975$ Å. All peak positions are in excellent agreement with bct, whereas fct fails to account for weak peaks at 2.965, 3.112, 3.31, and 3.85 Å^{-1}. bct is also more appealing on physical grounds, since adjacent Cs channels are staggered by $c/2$ which minimizes Coulomb repulsion. The intrachannel Cs-Cs separations are 3.975 and 3.642 Å for bct, and fct, respectively; again the bct choice minimizes Coulomb repulsion, while both are consistent with a standard Cs ionic diameter 3.4 Å. We point out that the intralayer Cs-Cs distance in graphite intercalates can be as short as 4.2 Å at 25 kbar hydrostatic pressure;[6] in this case the distance is imposed by $\sqrt{3}\times\sqrt{3}$ commensurate lock-in with the substrate. The film data of Ref. 4 show an intense (HKL) or (HHL) reflection at a Q value close to 1.7 Å^{-1}, providing further support for bct and ruling out any possibility that this peak is the trans-$(CH)_x$ (020)/(110).

The c parameter 3.975 Å implies that the Cs channels are incommensurate with the polymer chains at this doping level, assuming that the c-axis projected C-C distance remains at its undoped *trans*-$(CH)_x$ value 1.23 Å. The closest commensurate phase would have three (CH) units per Cs along the c axis ($y=0.167$); in our sample the Cs sublattice is 8% expanded along $\bar{c}$ with respect to this, implying a true $y=0.15$. (We have not attempted to determine y directly.) Dilation of the C—C bond due to charge transfer accounts for at most 2%.[7] In 2D systems an incommensurability this large usually produces "modulation peaks" whose wave vectors reflect the competing periodicities, orientational mismatch, domain walls, etc., but only if the coupling between the two sublattices is finite. Even the weak reflections in our data can all be accounted for by the pseudocell (see below), so we conclude that the c-axis correlations within a channel are entirely controlled by Cs^+-Cs^+ interactions. This aspect of $[(CH)Cs_{0.15}]_x$ is reminiscent of the incommensurate conductor $Hg_{2.86}AsF_6$,[8] although the Hg chains in the latter are completely decoupled in the two transverse directions while the Cs chains in the present case are strongly correlated in the (a,b) plane. The composite structure can be described as two interpenetrating 3D lattices which "float" with respect to each other along one axis. It is interesting to note that the graphite intercalation compound CsC_{24} exhibits both 3D incommensurate and 2D floating solid behavior in different regimes of hydrostatic pressure, the main effect of which is to modulate the coupling between graphite and Cs sublattices.[9]

In light of the above, we based our final analysis on a bct pseudocell in which each Cs channel is surrounded by four fictitiously dilated (CH) chains, producing an artificially commensurate structure with four Cs and 24 (CH) per cell; the c parameter is doubled to 7.952 Å since the cell must contain an even number of (CH) units. This can be referred to as a stage-1 phase by analogy to layer intercalates, since additional Cs could only be accommodated by increasing the number per unit length within a channel (a more-dense stage-1 structure in which the channels are defined by only three chains is found with smaller dopants, e.g., sodium[2]). The space group $P4_12_12$ is consistent with Ref. 4. Table I gives the calculated and measured d values and intensities, assuming full occupation of all sites and setting the thermal factors to zero. We tested the validity of the pseudocell approach by also calculating intensities for the Cs sublattice alone. Comparing the two I(calc) columns we see that interference between Cs and (CH) is only appreciable if H and K are even and $L=0$. All other intensities are sensitive to the *presence* of (CH) and thus are very well represented by the pseudocell model despite the wrong c-axis C-C spac-

TABLE I. Structural analysis of the profile in Fig. 1 based on a fictitiously commensurate pseudocell. Intensities are calculated both for the composite Cs+(CH) pseudocell structure and for the Cs sublattice alone (see text). The pseudocell parameters are $a=9.903$ Å, $\bar{c}=7.952$ Å; the space group is $P4_12_12$; there are six Cs and 24 (CH) per cell.

HKL	d(calc) (Å)	d(obs) (Å)	Q(obs) (Å^{-1})	I(calc) Cs only	I(calc) pseudocell	I(obs)
100	9.093			0	0	0
110	6.431	6.444	0.975	100	100	100
200	4.546	4.489	1.400	46	10	10
102	3.642	3.642	1.725	54	57	29
220	3.215	3.206	1.960	20	45	47
310	2.876			30	36	
212	2.843	2.856	2.200	59	62	53
302	2.410	2.407	2.610	19	20	5
400	2.273	2.267	2.772	8	15	6
330	2.143			7	5	
322	2.129	2.119	2.965	27	28	10
420	2.033			12	6	
004	1.988	2.019	3.112	3	3	4
412	1.928			20	21	
114	1.899	1.921	3.271	10	10	6
204	1.821			9	9	
510	1.783	1.795	3.500	8	7	4
224	1.690			7	7	
502	1.654			6	7	
432	1.654			13	13	
314	1.635	1.632	3.850	13	13	5
440	1.607			3	4	
530	1.559			6	8	
522	1.554	1.559	4.030	11	11	5
404	1.496	1.483	4.237	5	5	<2
334	1.457			5	5	
620	1.438			5	5	
424	1.421	1.430	4.395	8	9	4

ing. Furthermore, even (HKO) reflections which are affected by interference are only weakly dependent on the *difference* between actual and assumed c-axis (CH) periodicities since S(HKO) depends only on the (a,b) plane projection of the c-axis densities; the error in the (CH) contribution to I(calc) is thus the difference between actual and implied doping levels, so the overall error for these few reflections is $<10\%$.

The I(obs) values in Table I were obtained after background subtraction of a smoothly decreasing component and two broad peaks at 1.55 and 3.1 Å^{-1} representing the glass diffuse scattering. We estimate the accuracy of this procedure to be 2% of the largest I(obs). The overall agreement for d is excellent and for I is quite good (with significant exceptions discussed below). Despite the limited coherence length, the model accounts for all 27 predicted reflections in the Q range measured. Many of these are strongly overlapped, resulting in only 15 observed peaks. We find no measurable (100) intensity, which proves that the filling of the corner and center channels is rigorously the same.

We note from Table I that the (200) and (220) intensities agree with the respective I(calc)'s within experimental error, while I(obs) for (102) is only half I(calc). Also, the composite (310)/(212) intensity is consistent with the (212) being reduced to $\frac{1}{4}$ its ideal value. We thus suggest that the Debye-Waller factor for c-axis motion is significantly larger than the (a,b) plane component. This is borne out by examining the weaker peaks, especially the isolated (302) and (400) reflections for which I(obs)/I(calc)=0.25 and 0.4, respectively. Since the Debye-Waller factor varies as $\exp(-Q^2u^2)$, the high-Q peaks should show the largest discrepancies. Indeed the quadruplet at $d=1.632$ Å contains only finite L components and I(obs)/I(calc)=0.12, while the 1.559-Å triplet, for which only one of three components has nonzero L, shows a smaller effect: I(obs)/I(calc)=0.2. Similarly, the (404) is barely visible in reflection [Fig. 1(b)]. These systematic effects must be due to an anisotropic Debye-Waller factor; local disorder (if any) would have to affect equally the (H,K) and (L) components of $S(Q)$, since the correlation length happens to be isotropic. $S(Q)$ itself is dominated by Cs, so we conclude that the amplitude of Cs thermal motion within a channel is larger than the transverse amplitude. This is consistent with the apparent decoupling of Cs channels and (CH) chains in defining the static structure.

Our results agree generally with Ref. 4, in which highly oriented $(CH)_x$ was vapor doped with K, Rb, or Cs. The two sets of lattice constants for $[(CH)Cs_y]_x$ differ

significantly; our $\bar{a}$ value is 0.8% larger and $\bar{c}$ is 3.7% smaller. Differences in $\bar{c}$ almost certainly reflect different y values; the Cs-(CH) interaction seems to be negligible, so the pseudo-c parameter is controlled entirely by Cs-Cs interactions and probably varies continuously over a limited range of y. The (smaller) disagreement in $\bar{a}$ is more interesting. For $[(CH)K_y]_x$, our *in situ* x-ray data showed a 2.4% increase in $\bar{a}$ accompanying the stage-2→stage-1 transition,[3] a steric effect associated with the filling of the second set of channels (see below). Thus the smaller $\bar{a}$ value in Ref. 4 could be attributed either to a small admixture of stage-2 or to a new phase with slightly different Cs occupancies in the two sets of tunnels. Both possibilities would imply finite (100) intensity, which is difficult to assess from the film data. The disagreement in $\bar{a}$ may not be significant, but in any event it would be interesting to study the structural evolution continuously with y, in particular to see if there are any consequences of commensurate lock-in at rational (CH)/Cs ratio.

The alkali metals K, Rb, and Cs all form centered tetragonal arrays of dopant channels in $(CH)_x$, each channel being defined by four (CH) chains in a square array.[4] It is now well established (at least for K doping) that the structural evolution with increasing y proceeds via selective filling of first one (e.g., corner) then the other (e.g., center) channel, analogous to stage 2 and stage 1 in graphite intercalation compounds.[3] Elastic interactions play a major role in stabilizing high stages in graphite,[10] so it may be informative to consider the doping-induced dilation of $(CH)_x$. In Table II we compare the average c-axis separation per C layer with the average (a,b) plane separation of a (CH) chain (the former is simply the repeat distance divided by the number of C layers per repeat, while the latter is the square root of the basal plane area per chain). Note first that the fractional c-axis dilation accompanying the formation of stage-2 K graphite far exceeds the corresponding quantity for $(CH)_x$, 31% versus 5%. It has long been recognized that twisting of the chains plays a major role in "preparing" the channels for intercalation, and that the twisting *per se* causes $\bar{b}$ to expand while $\bar{a}$ actually contracts.[1] Secondly, the stage-2→stage-1 transition in K graphite imposes an additional 30% dilation, while for $(CH)_x$ the additional dilation is only 2%; in the latter case all the channels are already "prepared" at stage-2 even though only half are occupied. One common feature does emerge, namely the influence of atomic size; replacing K by Cs in the stage-1 structures leads to linear expansions of 10% and 8%, respectively, indicating that guest-host hybridization is either negligible or comparable in both intercalate families.

Both for doped polymers and layer intercalates, high stages are energetically favored if y is less than the saturation value and $U_0 \gg kT$, where U_0 is a short-range attractive interaction between dopants in the same channel or gallery.[11] The physical origin of U_0 is thought to be local distortions of the host lattice surrounding isolated dopants; U_0 scales as z/L^2, where z is the transverse dilation and L is the longitudinal healing length.[10] For layer intercalates z is determined by the c-axis dilation and L can be estimated from the y dependence of the c parameter in the high-T limit. This approach successfully explains why Li_yC_6 shows high stages at 300 K while Li_yTiS_2 does not; the z's are the same but the stiffer host "layers" in the latter lead to a larger L, hence smaller U_0. According to Table II the analogous procedure for doped polymers may be considerably more difficult; local distortions around an isolated dopant in $(CH)_x$ will consist of both single-chain twisting and chain-chain dilation, and the energetics will certainly be dominated by the former. On the other hand, much can be and has been learned about local elastic effects in layer intercalates from studying stage-1 ternary compounds, e.g., $K_yCs_{1-y}C_8$.[12] Table II shows that the size effects are similar in graphite and $(CH)_x$, suggesting that studies of ternary polyacetylene phases might be similarly fruitful.

TABLE II. Comparison of the average linear dilation induced by K or Cs doping and by staging transitions in graphite and polyacetylene.

	Graphite	Polyacetylene
Undoped	3.35	3.92
K doped		
stage 2	4.38	4.10
stage 1	5.40	4.20
(K undoped)/undoped		
stage 2	0.31	0.05
stage 1	0.61	0.07
Cs doped		
stage 1	5.94	4.55
(Cs-K)/K	0.100	0.08

We acknowledge helpful discussions with Paul Heiney and Siegmar Roth, and the experimental assistance of Stefan Idziak. We are grateful to Michele LeLaurain for sharing an early version of Ref. 4 with us. This research was supported by the National Science Foundation Materials Research Laboratory Program Grant No. DMR85-19059 (J.E.F., J.M.), and by U.S. Department of Energy Grant No. DEFG02-87ER45254 (D.D.). The Penn-Montpellier collaboration is supported by NATO Grant No. 0866/87.

*Also at Department of Physics, University of Pennsylvania, Philadelphia, PA 19104.

†Present address: Laboratoire de Chimie des Solides, Universite Blaise Pascal, Clermont-Ferrand, France.

‡Also at Department of Materials Science and Engineering, University of Pennsylvania, Philadelphia, PA 19104.

[1] L. W. Shacklette, J. E. Toth, N. S. Murthy, and R. H. Baughman, J. Electrochem. Soc. **132**, 1529 (1985).

[2] M. J. Winokur, Y. B. Moon, A. J. Heeger, J. Barker, D. C. Bott, and H. Shirakawa, Phys. Rev. Lett. **58**, 2329 (1987).

[3] D. Djurado, J. E. Fischer, P. A. Heiney, J. Ma, N. Coustel, and P. Bernier, Synth. Metals (to be published).

[4]F. Saldi, J. Ghanbaja, D. Begin, M. LeLaurain, and D. Billaud, C. R. Acad. Sci. (to be published).
[5]F. Rachdi and P. Bernier (private communication).
[6]C. D. Fuerst, J. E. Fischer, J. D. Axe, J. B. Hastings, and D. B. McWhan, Phys. Rev. Lett. **50**, 357 (1983).
[7]N. S. Murthy, L. W. Shacklette, and R. J. Baughman, J. Chem. Phys. **87**, 2346 (1987); M. J. Winokur, Y. B. Moon, A. J. Heeger, J. Barker, and D. C. Bott, Solid State Commun. **68**, 1055 (1988).
[8]J. B. Hastings, J. P. Pouget, G. Shirane, A. J. Heeger, N. D. Miro, and A. G. MacDiarmid, Phys. Rev. Lett. **39**, 1484 (1977).
[9]N. Wada, S. Minomura, and J. Pluth, Synth. Metals **12**, 51 (1985).
[10]J. E. Fischer and H. J. Kim, Phys. Rev. B **35**, 3295 (1987).
[11]J. Ma, H.-Y. Choi, E. J. Mele, and J. E. Fischer, Synth. Metals **27**, A75 (1988).
[12]S. Lee, H. Miyazaki, S. D. Mahanti, and S. A. Solin, Phys. Rev. Lett. **62**, 3066 (1989).